



# Flow Cytometric Ploidy Analysis in Acute Lymphoblastic Leukemia and Plasma Cell Myeloma

Karthik Bommannan<sup>1</sup>

<sup>1</sup>Department of Oncopathology, Cancer Institute (W.I.A.), Adyar, Tamil Nadu, India

Address for correspondence Dr. Karthik Bommannan B.K. Department of Oncopathology, Cancer Institute (W.I.A.) Adyar, Chennai, Tamil Nadu 600020, India (e-mail: bkkb87@gmail.com).

Ind J Med Paediatr Oncol 2023;44:525–533.

## Abstract

Identification of underlying cytogenetic (CG) aberrancies plays a significant role in risk stratification of hematological malignancies. These abnormalities can be due to aberrancies that affect the number or structure of chromosomes. Numerical chromosomal abnormalities are called aneuploidies, which result from either gain or loss of whole chromosomes. Ploidy assessment by CG is a laborious and less sensitive technique. With the aid of fluorescent nucleic acid binding dyes, the total DNA content and different phases of the cell cycle specific to any population of interest can be deciphered and analyzed by flow cytometry (FCM). DNA index (DI), a parameter derived by FCM DNA analysis, is equivalent to conventional CG-based ploidy assessment. In this study, the technical aspects and implications of FCM DNA assessment among patients diagnosed with acute lymphoblastic leukemia and plasma cell myeloma are discussed.

## Keywords

- ▶ ploidy
- ▶ flow cytometry
- ▶ DNA Index
- ▶ S-phase fraction

## Introduction to Cell Cycle

Cell cycle is a strictly regulated sequential series of events that result in two offspring cells from a single parent cell. Cells enter into a cell cycle in response to either biological or pathological stimuli.<sup>1</sup> Until such stimuli occur, the cells remain in a dormant phase called the G<sub>0</sub> phase. The sequential series of events in a cell cycle is described in ▶ **Table 1** and the techniques available to assess the cell cycle are described in ▶ **Table 2**.

## Concept of Flow Cytometric Cell Cycle Analysis

The cells in G<sub>0</sub>/G<sub>1</sub> (pre-replicative), S (replicative), and G<sub>2</sub>/M (post-replicative) phases differ by their intracellular DNA content. Flow cytometry (FCM) can segregate these cells based on the amount of fluorescent DNA binding dye present in each cell.<sup>2–5</sup>

## Fluorescent Nucleic Acid Binding Dyes

These dyes emit fluorescence upon binding to their nucleic acid targets.<sup>6</sup> To be eligible for FCM DNA analysis, a fluorescent dye must fulfill the following prerequisites<sup>6</sup>:

- It must have specific binding to nucleic acids.
- It must acquire strong fluorescence after binding to its nucleic acid target.
- The dye's fluorescence emission must be stoichiometric to the target cell's nucleic acid content.
- The dye must have preferential binding to either DNA or RNA. Dyes that have an equal affinity to both DNA and RNA are less preferred. However, undesired but minimal RNA binding in DNA preferential dyes can be overcome by RNase treatment.

Commonly used dyes for FCM-based nucleic acid analysis and their preferential DNA and RNA binding properties are

DOI <https://doi.org/10.1055/s-0043-1776046>.  
ISSN 0971-5851.

© 2023. The Author(s).

This is an open access article published by Thieme under the terms of the Creative Commons Attribution License, permitting unrestricted use, distribution, and reproduction so long as the original work is properly cited. (<https://creativecommons.org/licenses/by/4.0/>)  
Thieme Medical and Scientific Publishers Pvt. Ltd., A-12, 2nd Floor, Sector 2, Noida-201301 UP, India

**Table 1** Sequential stages of cell cycle and intracellular events at each stage<sup>53</sup>

Interphase	Phase	Intracellular events
	G0	<ul style="list-style-type: none"> <li>• Dormant stage between two cell cycles</li> <li>• Cells perform their physiological function, but there is no synthesis of RNA and ribosomal protein machinery needed for DNA synthesis</li> </ul>
	G1	<ul style="list-style-type: none"> <li>• Time gap between a recently concluded mitosis and the onset of the next DNA synthesis process</li> <li>• Cells undergo synthesis of RNA and ribosomal protein machinery needed for DNA synthesis</li> </ul>
	S	<ul style="list-style-type: none"> <li>• Synthesis and replication of nuclear DNA content before division</li> <li>• Indicates proliferative intent of a cell</li> </ul>
	G2	<ul style="list-style-type: none"> <li>• The interval between completion of DNA synthesis and onset of mitosis</li> <li>• Opportunity to repair any DNA damage that might have occurred in preceding cell cycles</li> <li>• Reorganization of DNA structure, enabling equal division of DNA between ensuing daughter cells</li> </ul>
Mitosis	M	<ul style="list-style-type: none"> <li>• The actual process of cell division</li> <li>• Equal distribution of DNA, RNA, protein, and cellular organelles between the daughter cells</li> </ul>

**Table 2** Laboratory techniques to assess cell cycle

Technique		Brief Description
Immunohistochemistry-based cell cycle detection (iCCD) <sup>53,54</sup>		<ul style="list-style-type: none"> <li>• Geminin: Highest expression in S/G2/M phase and degrades after M phase</li> <li>• Chromatin licensing and DNA replication factor 1 (Cdt1): Highest expression in G1 phase and degrades before S phase</li> <li>• Gamma H2A.X: Marker for DNA double-strand breaks (DSBs)<sup>55</sup></li> </ul>
Fluorescence in situ hybridization (FISH) <sup>56</sup>		<ul style="list-style-type: none"> <li>• Ploidy assessment by centromere and <math>\alpha</math>-satellite DNA assessment probes</li> </ul>
Fluorescent ubiquitination-based cell cycle indicator (FUCCI) <sup>57</sup>		<ul style="list-style-type: none"> <li>• Fluorescence-labelled proteins tagged with Cdt 1 and Geminin</li> <li>• Time-lapse photographs are used to identify both temporality and spatial organization of cells in culture according to their stage in cell cycle</li> </ul>
Radioisotope-labeled DNA <sup>58</sup>		<ul style="list-style-type: none"> <li>• Incorporating radioisotope (now replaced by nucleoside analogues) into the DNA to calculate the time spent by a cell across the cell cycle stages</li> </ul>
Flow cytometry <sup>2,3,8,9,52</sup>	Univariate	<ul style="list-style-type: none"> <li>• Using DNA binding dyes that enable only cellular DNA content assessment</li> <li>• Applicable in samples that have only/predominantly tumor cells</li> </ul>
	Bivariate	<ul style="list-style-type: none"> <li>• Combined use of a DNA binding dye along with another dye/antibody specific to RNA, cyclins, or cell proliferation-related antigens (e.g., Ki67)</li> <li>• Enable better understanding of cell cycle kinetics</li> </ul>
	Multivariate	<ul style="list-style-type: none"> <li>• Combination of cell surface antigen and intracellular DNA staining</li> <li>• Cell surface antigens aid in gating cells of interest, enabling cell population-specific DNA analysis</li> </ul>
Mass flowcytometry (FCM) <sup>59</sup>		<ul style="list-style-type: none"> <li>• Combination of conventional FCM and mass spectrometry</li> <li>• Metal-labeled antibodies specifically bind to the proteins to be detected</li> <li>• Enables concurrent detection of multiple metal-labeled antibody-antigen complexes by mass spectrometry, facilitating simultaneous analysis of more than 40 antigens per cell</li> </ul>
Microfluidics-based cell cycle analysis <sup>60</sup>		<ul style="list-style-type: none"> <li>• Detecting intracellular DNA content and cell cycle-specific proteins</li> <li>• Can be performed on low-volume samples</li> </ul>
Raman spectroscopy <sup>61</sup>		<ul style="list-style-type: none"> <li>• Label-free technique for cell cycle analysis</li> <li>• Functional capability of cells is retained</li> </ul>
Cell cycle chromobody (CCC) <sup>62</sup>		<ul style="list-style-type: none"> <li>• Uses fluorescent protein-linked intracellular functional single-domain antibody</li> <li>• Demonstrates cell cycle-dependent distribution of proliferating cell nuclear antigen (PCNA) in living cells</li> </ul>

depicted in ► **Supplementary Table S1** (available in the online version).

## Components of DNA Histogram

In FCM, the cell cycle is analyzed as a frequency histogram where the fluorescence intensity of DNA binding dye and the number of cells is plotted across the X-axis and Y-axis, respectively.<sup>4</sup> In a cell cycle histogram, the fluorescence intensity of DNA binding dyes is expressed in a linear scale. The linear scale simplifies interpretation of DNA histogram as each unit in this scale represents an equal interval in increments of fluorescence (i.e., DNA content per cell). As the data is well spread in a linear scale, individual phases of cell cycle can be grossly identified by visual inspection itself. Also, the linear scale facilitates identification of artefacts and sub-G0/G1 peaks, which might be readily missed in a log-scale.

Due to the stoichiometric binding of DNA-specific dyes, all cells in any given phase of the cell cycle are expected to have the same amount of DNA and the “expected” cell cycle must be as the green, blue, and red colored bars depicted in ► **Fig. 1**. However, due to cell-to-cell variability in dye binding, a gaussian curve with normal distribution is generated for each phase of the cell cycle, and a multimodal histogram is generated as depicted in ► **Fig. 1**.

Following are the components of a DNA histogram. The *G1/G0 curve* represents cells in G0/G1 phases of the cell cycle. Using DNA-specific dyes, a distinction between G0- and G1-phase cells is not feasible as both G0- and G1-phase cells have the same DNA content. In contrast to G0 cells, which have only DNA, cells in the G1 phase also have RNA (refer ► **Table 1**). Combined use of RNA binding dyes like pyronin Y along with a DNA-specific dye (having a different emission spectrum) can aid distinction between G0- and G1-phase cells. The *G2/M curve* represents cells in the G2/M

phase of cell cycle. In theory, the G2/M-phase cells must have exactly double the DNA content of cells in the G0/G1 phase. However, the extensive DNA-protein interactions in the G2/M-phase cells result in extensive chromatin compaction, which hinders stoichiometric nucleic acid binding by the dyes. Due to this, the dye fluorescence intensity of cells in the G2/M phase is 1.97 times that of the cells in the G0/G1 phase.<sup>7</sup> The *S curve* is a broad-based histogram between G0/G1 and G2/M curves. This curve reflects the gradual increase in the DNA content of a cell until it reaches a content equivalent to a cell in the G2/M phase.

In a DNA histogram, the “origin point” indicates the point on x-axis where the fluoresce of the DNA binding dye starts. In a typical DNA histogram, the peak starting from this origin point has the least DNA content, that is, the G0/G1 peak. This origin point on the x-axis must be clearly defined in the DNA histogram as it facilitates data normalization for comparing DNA histograms from different experiments or samples or different cell populations within the same sample. The origin point is also the end result of variations in sample age, sample processing, and measurement techniques. The exact start and end points of G1/G0, S, and G2/M histograms are always arbitrary by manual gating. To identify the correct proportion of cells representing each phase of a cell cycle, mathematical modeling-based curve fitting algorithms are available (Dean-Jett model of 1974, Fox-modified Dean-Jett model of 1980, Watson’s pragmatic model of 1987, etc.).

## Clinically Relevant Parameters Derived from FCM DNA analysis

In patients diagnosed with B-lineage acute lymphoblastic leukemia (B-ALL) and plasma cell myeloma (PCM), the DNA index (DI) and S-phase fraction (SPF) are the two parameters of clinical relevance obtained by FCM DNA analysis.

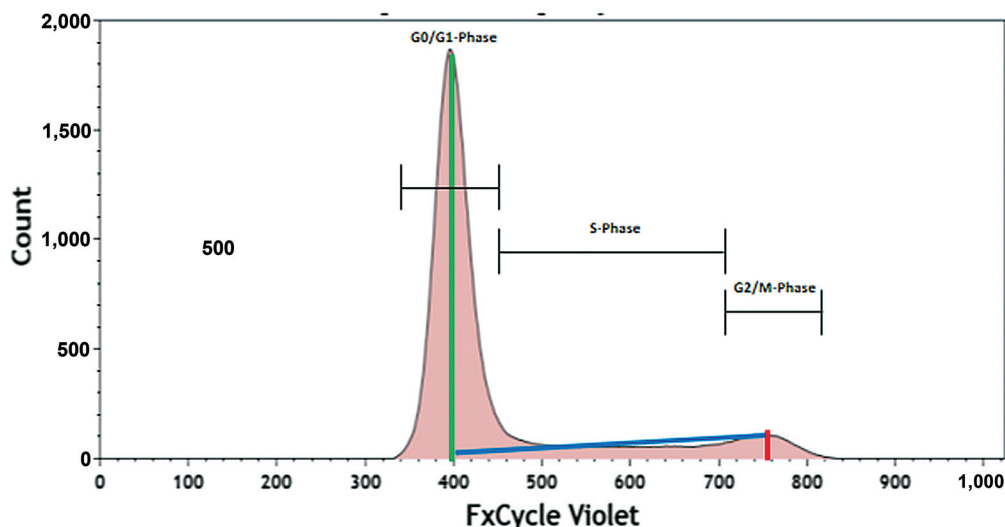


**Fig. 1** Flowcytometric DNA assay depicted as a multimodal histogram (shaded curves). The green, blue, and red colored lines represent the theoretical G0/G1, S, and G2/M phases, respectively. Y-axis: number of cells. X-axis: intensity of staining with FxCycle violet, a DNA-specific fluorescent dye.

## DNA Index

The DI is calculated as the ratio of the G<sub>0</sub>/G<sub>1</sub> phase of malignant cells to that of the G<sub>0</sub>/G<sub>1</sub> phase of normal diploid control cells.<sup>4</sup> There is near 90% correlation between the ploidy status assessed by DI and cytogenetics (CG).<sup>8–10</sup> There are published cutoffs (refer to ► **Supplementary Table S2**, available in the online version) that have correlated the range of DI with the corresponding number of chromosomes in a population of cells.<sup>8,11–13</sup> The advantages of ploidy assessment by DI are that the technique is more rapid and sensitive than CG, and can aid in ploidy identification even in samples with less than 1% cells of interest.<sup>8</sup> This technique can identify cell population-specific ploidy even in samples with markedly heterogeneous cellular composition (e.g., bone marrow). However, ploidy evaluation by FCM is not sensitive in assessing aneuploidies involving smaller chromosomes.<sup>9</sup>

## Role of DNA Index in B-Lineage Acute Lymphoblastic Leukemias

Hyperdiploidy (51–65 chromosomes) is observed in nearly 30% of pediatric patients diagnosed with B-ALL and is associated with a favorable prognosis.<sup>14–16</sup> These hyperdiploid blasts are highly susceptible to apoptosis and hence require stringent conditions for their ex vivo survival. This is reflected in frequent metaphase failures and/or poor morphology of chromosomes during conventional CG evaluation of these patients. Under ambient culture conditions used for conventional karyotyping, the normal diploid cells in the sample can overwhelm the hyperdiploid blasts and result in pseudodiploidy. Ploidy assessment by DI is effective in overcoming these limitations of conventional CG-based ploidy assessment.

The relevance of DI in pediatric patients with B-ALL was observed as early as 1985.<sup>17</sup> A DI of  $\geq 1.16$  in these patients is consistently associated with hyperdiploidy and hence better outcomes.<sup>11,13,17–21</sup> Although there is more than 95% concordance in hyperdiploidy identified by DI and karyotyping, not all B lymphoblasts with 51 to 65 chromosomes have DI  $\geq 1.16$ .<sup>8,9,22</sup> In this context, it has been proposed to consider B lymphoblasts having 51 to 55 chromosomes and DI of 1.10 to 1.15 as “low DI-high hyperdiploid” (LDI-HHD). These patients with LDI-HHD have a poor prognosis as compared to patients with DI  $\geq 1.16$  and 51 to 65 chromosomes, that is, the “high DI-high hyperdiploid” category.<sup>23</sup> In fact, patients with DI  $\geq 1.24$  (corresponding  $\geq 58$  modal chromosomes) have the best prognosis.<sup>23</sup> ► **Fig. 2** demonstrates the FCM DNA analysis histograms of individual patients with diploid (► **Fig. 2a–c**) and hyperdiploid (► **Fig. 2d–f**) B lymphoblasts.

Hypodiploidy (<46 chromosomes) is observed in less than 5% of pediatric B-ALL patients.<sup>15</sup> In this category, patients with 31 to 39 chromosomes (low hypodiploid) and 24 to 29 chromosomes (near haploid) have dismal prognosis.<sup>15,24,25</sup>

Endoreduplication is a phenomenon where a cell undergoes DNA replication without undergoing cell division.<sup>24</sup> This results in the cell having multiple copies of its chromosomes within a single nucleus. Although endoreduplication is a physiological process in certain human cells (e.g., megakaryocytes), its occurrence in blasts is pathological and complicates ploidy assessment.<sup>24</sup> Nearly 65% of patients with near haploidy and 45% of patients with low hypodiploidy undergo endoreduplication.<sup>24</sup> Due to this phenomenon, CG can misinterpret endoreduplicated near-haploid and

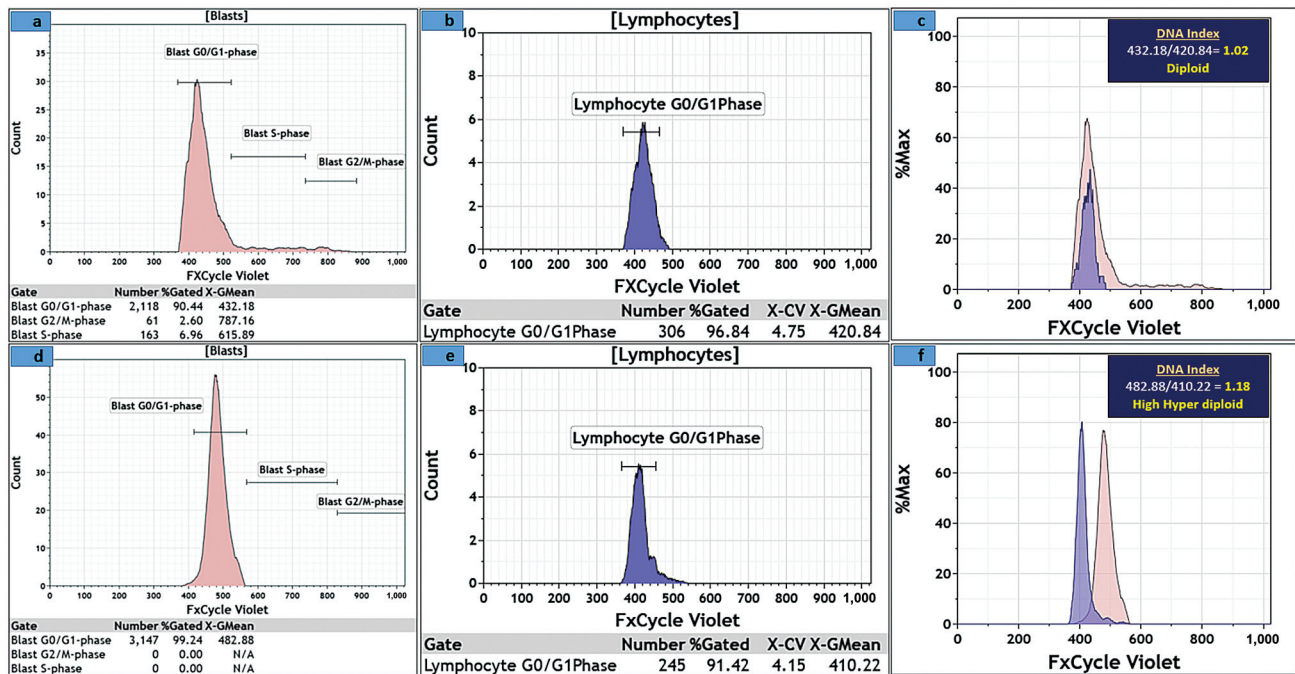


**Fig. 2** DNA index assessment in B-lymphoblastic acute lymphoblastic leukemia using FxCycle violet, a DNA-specific dye. (a–c) From a sample with diploid blasts. (d–f) From a sample with high hyperdiploid blasts. Overlay histograms (c,f) show the G<sub>0</sub>/G<sub>1</sub>-phase cells of both blasts and lymphocytes. The fluorescence intensity of FxCycle violet is depicted as Geometric mean (GMean) of expression.

low-hypodiploid lymphoblasts as hyperdiploid (50–60 chromosomes) and near-triploid (up to 78 chromosomes) lymphoblasts, respectively.<sup>24</sup> Recently, both low-hypodiploid and near-triploid blasts have been recognized as a unified genetic entity involving *TP53* mutations.<sup>24–26</sup> Hence, misinterpretation of low hypodiploidy as near triploidy might not affect the patient's prognosis. However, misclassification of endoreduplicated near haploidy as high hyperdiploidy is detrimental.<sup>24</sup> In a sample where the near-haploid blasts have endoreduplicated, the ensuing hyperdiploid blasts are larger in size than their founder cell.<sup>24–27</sup> Using blast size-specific DI assessment, both hypodiploid and endoreduplicated hyperdiploid blasts in a sample can be identified in isolation.<sup>9</sup>

### Role of DNA Index in Plasma Cell Myeloma

Malignant plasma cells in nearly 50% of patients with PCM are hyperdiploid due to trisomies involving odd-numbered chromosomes.<sup>28–32</sup> These hyperdiploid PCM patients have a better prognosis as compared to hypodiploid and *IgH* translocated PCM patients.<sup>33,34</sup> As plasma cells are terminally differentiated, conventional CG results in normal diploid metaphases (possibly of myeloid origin) in nearly 70% of PCM samples.<sup>34</sup> In this context, a multiparametric FCM DI analysis can identify ploidy in both normal and malignant plasma cells.<sup>10,35</sup> Using normal plasma cells as the reference population, malignant plasma cells with DI of 0.95 to 1.05, 1.06 to 1.50, 1.51 to 1.70, and greater than 1.71 are considered diploid, hyperdiploid, near tetraploid, and tetraploid, respectively.<sup>35</sup> Using lymphocytes as diploid control, an alternative cutoff of  $\leq 0.95$  (hypodiploid), 0.95 to  $\leq 1.05$  (diploid), 1.06 to 1.15 (near hyperdiploid), and  $\geq 1.16$  (hyperdiploid) to define DI-based ploidy has also been described.<sup>10</sup>

### S-Phase Fraction of Malignant Cells

In a cell cycle, cells in the S phase are those that undergo active DNA replication (refer to ►Table 1). As cells in the S phase eventually result in mitosis (i.e., physical doubling of the cells), the SPF reflects the proliferative capability of the tumor.

### Role of S-Phase Fraction Assessment in Acute Lymphoblastic Leukemias

The relevance of SPF assessment in acute leukemias dates back to 1980 when the presence of greater than 6% lymphoblasts in the S phase was associated with poor prognosis among pediatric patients diagnosed with ALL.<sup>36</sup> This 6% cutoff was established based on the median SPF (range of 1–60% and mean of 9%) among 65 ALL samples with greater than 80% lymphoblasts, irrespective of their B- or T-lineage origin.<sup>36</sup> The prognostic relevance of this 6% SPF was further confirmed by contemporary literature from both the Dutch and British groups.<sup>11,36</sup> However, further literature regarding the relevance of SPF in pediatric patients with ALL is sparse and has not claimed any prognostic relevance.<sup>18,37,38</sup> Due to the emergence of more robust risk assessment modalities, SPF is no longer used as a prognostic tool in any present-day pediatric ALL treatment protocols.

### Role of S-Phase Fraction Assessment in Plasma Cell Myeloma

The proliferative capability of plasma cells, as indicated by the plasma cell labeling index (PCLI), is a time-tested prognostic factor in patients diagnosed with plasma cell dyscrasias.<sup>39</sup> Initial PCLI identification assay using radiolabeled thymidine incorporation followed by autoradiography was both technically challenging and hazardous. In 1985, PCLI by a smear-based immunofluorescence assay utilizing an anti-5-Bromo-2'-deoxyuridine (BrdU) antibody was introduced. A PCLI of less than 1, 1 to 3, and  $\geq 3\%$  identified by this technique was associated with low, intermediate, and high-risk diseases, respectively.<sup>40–44</sup> Although this BrdU-based PCLI technique is safer and relatively easier than the radio-labeled thymidine technique, it is not widely utilized in routine practice.<sup>39</sup>

In 1994, Orfão et al described an FCM-based CD38/propidium iodide dual staining technique to analyze the DNA content of plasma cells in the bone marrow of patients diagnosed with PCM.<sup>45</sup> According to that study conducted among 120 treatment naïve PCM patients, those patients with  $\geq 3\%$  malignant plasma cells in the S phase had inferior relapse-free and overall survival.<sup>30</sup> To date, higher SPF of malignant plasma cells identified by FCM is considered one of the parameters associated with high-risk disease across the spectrum of plasma cell dyscrasias and at various phases of treatment.<sup>39,46–48</sup>

### Laboratory Aspects of Flow Cytometric Ploidy Assessment

A successful FCM DNA analysis warrants fulfilling of the prerequisites discussed in the following sections.

#### Sample-Related Prerequisites

FCM DNA analysis pertinent to hematological malignancies is commonly performed on fresh, unfixed, fluid-state samples like peripheral blood, bone marrow, body fluids, and fine needle aspirates.<sup>18</sup> In indications requiring sample fixation (like transported samples), precipitating fixatives (acetone and alcohol) are preferred over cross-linking fixatives (formaldehyde and glutaraldehyde).<sup>4</sup> This is because the nucleic acid cross-linking resulting from these fixatives will interfere with the desired stoichiometric binding of the dyes.<sup>4</sup> In the era of univariate and bivariate FCM DNA analysis, it was recommended to perform the assay in samples with a minimum of 15 to 20% malignant cells of interest.<sup>49</sup> With the advent of multiparametric FCM DNA analysis, the assay could be successfully performed even in samples with less than 1% malignant cells.<sup>8</sup>

If the assay has to be performed on archived paraffin blocks, the following factors have to be taken care of. A cell suspension must be prepared from a section of the paraffin block that contains both the tumor cells and normal resident cells (selected by light microscopic evaluation). The thickness of the section is determined by the size of the tumor cell's nucleus (a 50-nm-thick section would be optimal).<sup>5</sup> The quality of DNA binding dye staining is relatively inferior as the tissue is already exposed to formaldehyde during



**Table 3** Common issues encountered during flow cytometric DNA analysis and the possible reasoning and solutions to consider

Issue	Reasons	Solution
Doublets and cell aggregates	Higher relative centrifugal force (RCF)	The ideal RCF has to be calculated to achieve an optimal centrifugation force of 500–540 $g$ <sup>52</sup>
	Aged sample. Autolysis of cells cause release of sticky nuclear content, causing cell-to-cell adhesions	Sample should be processed as fresh as possible, ideally within 24–48 h from collection <sup>52</sup>
	Sample acquired at high acquisition rate	The sample must be acquired at a low event rate, ideally 100–200 events/s <sup>52</sup>
	Harsh handling of samples during processing	Mixing steps involved during processing must be gentle, preferably using a Pasteur pipette <sup>52</sup>
Nonstoichiometric staining (ideally >90% cells in a sample must be stained with the dye) <sup>52</sup>	Low concentration of dye used for staining	Re-standardize the assay with gradients of dye concentration to identify optimal dye concentration to be used. Note: the cell concentration and incubation time have to be kept constant
	Excess of cells in the cell suspension being stained	Re-standardize the assay with gradients of cell concentrations to identify optimal cell concentration to be used. Note: the dye concentration and incubation time have to be kept constant
	Insufficient incubation time	Re-standardize the assay with gradients of incubation time to identify optimal incubation time. Note: the dye and cell concentration have to be kept constant
	Samples from patients on DNA binding anticancer drugs	Repeat the assay in a treatment naïve sample (if available)
Undesired RNA binding <sup>4</sup>	The degree of undesired RNA binding depends on the dye's RNA binding propensity	<ul style="list-style-type: none"> <li>• While using dyes with higher RNA binding propensity (e.g., propidium iodide), the sample has to be treated with RNase before incubation with the dye<sup>4</sup></li> <li>• A dye without RNA binding capability (e.g., FxCycle violet) can be used<sup>9,52</sup></li> </ul>
Sub-G0/G1 population <sup>4</sup> (the cells that have DNA content less than that of a normal diploid control)	Apoptosis: apoptosis results in DNA fragmentation of specific lengths. During sample processing, apoptotic cells leak out their intracellular contents (including smaller DNA fragments). Hence, apoptotic cells have a lower total DNA content than normal diploid control and manifest as a distinct sub-G0/G1 peak	<ul style="list-style-type: none"> <li>• If a sub-G0/G1 peak is also present in diploid controls, then the sub-G0/G1 population present in the malignant cells can be considered apoptotic and ignored; however, this approach is subjective and risks exclusion of true hypodiploid malignant cells<sup>9</sup></li> <li>• Concurrent staining with annexin V will aid objective identification of apoptotic cells<sup>9</sup></li> </ul>
	Necrosis: necrosis involves random-sized DNA fragmentation, resulting in a sub-G0/G1 “smearing pattern” against a perfect peak generated by apoptosis/hypodiploid cells	Samples should be fresh and processed within 24–48 h of collection <sup>52</sup>

fixation; hence, stoichiometric staining might not be optimal.<sup>3,4</sup> In this scenario, 4',6-diamidino-2-phenylindole (DAPI) is the preferred nucleic acid binding dye as it is least affected by formaldehyde-induced cross-linking.<sup>4</sup> Since the nucleus of cells is cut through during sectioning, it is common to get a sub-G0/G1 population during analysis. This population must not be interpreted as a hypodiploid clone of cells. In such situations, curve-fitting algorithms/software

(Dean–Jett model of 1974, Fox-modified Dean–Jett model of 1980, Watson's pragmatic model of 1987, MultiCycle of 1988, etc.) can be used to analyze the cell cycle.

#### Assay-Related Prerequisites

For any FCM DNA assay, it is mandatory to validate the linearity, degree of resolution, and robustness of sample processing in a machine and panel-specific setting. Commercially

available chicken or trout (they inherently have a mixture of single, double, triple, and quadruple nucleated red blood cells [RBCs]) erythrocytes are used for this purpose.<sup>4,10</sup>

According to the 1993 DNA cytometry consensus conference's recommendations, indigenous normal cells (stromal cells in the case of paraffin-embedded tissues) present in a tumor-rich sample should be used as internal diploid controls. In scenarios where such internal controls are not available/sparsely present within the sample, normal diploid cells sourced from healthy controls can be spiked to the tumor sample before processing.

In the context of FCM DNA analysis pertinent to hematological malignancies, lymphocytes are used as diploid controls. Neutrophils and monocytes are not ideal controls as the former are highly fragile and the latter have increased stainability (especially for propidium iodide) due to their unique chromatin conformation.<sup>4</sup>

### Sample Processing–Related Prerequisites

The protocols pertinent to sample processing toward FCM DNA analysis depend on the nature of the sample, the cell-permeant ability of the dye, and its extent of RNA binding capability (refer to ► **Supplementary Table S1**, available in the online version). Detailed discussion regarding the specific modifications required for each dye is beyond the scope of this review but is readily available in the literature.<sup>2,3,50,51</sup> The vital features are that the samples must be processed within 24 to 48 hours of collection. A stable dye binding equilibrium is achieved only if the concentration of dye used for staining is nearly 100 times above the concentration of the cells to be stained. Hence, the optimal concentrations of cells and the dye used must be standardized to achieve stoichiometric staining.<sup>52</sup> The processed samples must be acquired immediately and the acquisition must be at a low event rate, around 100 to 200 events per second.<sup>52</sup> A minimum of 200 diploid control cells must be acquired.<sup>52</sup>

### Analysis-Related Prerequisites

For optimal FCM DNA evaluation, a minimum of 90% of cells must be stained with the DNA binding dye.<sup>52</sup> The quality of an FCM DNA assay is evaluated based on the coefficient of variation (CV) of the G0/G1 phase of diploid control cells present in the processed sample. This CV is the result of sample quality, sample processing errors, heterogeneity in individual cells' DNA content, and the degree of chromatin compaction. For optimal FCM DNA analysis, the CV of the G0/G1 phase of diploid control must be less than 6%, with CV less than 3% yielding the best results.<sup>4,18,52</sup>

The common pitfalls encountered during FCM DNA analysis are depicted in ► **Table 3**.<sup>3,4,52</sup>

## Conclusion

FCM DNA assessment is an objective, reproducible, and sensitive assay to evaluate ploidy and SPF of any cells of interest. FCM-determined ploidy correlates with CG-determined ploidy and patient survival. The FCM DNA assay can be used even in scenarios where the load of tumor cells is low or conventional CG assessment is not feasible or fails.

### Funding

None.

### Conflict of Interest

None declared.

## References

- 1 Clurman BE, Roberts JM. Cell cycle and cancer. *J Natl Cancer Inst* 1995;87(20):1499–1501
- 2 Darzynkiewicz Z, Juan G, Bedner E. Determining cell cycle stages by flow cytometry. *Curr Protoc Cell Biol* 1999;1(01):8.4.1–8.4.18
- 3 Darzynkiewicz Z, Huang X, Zhao H. Analysis of cellular DNA content by flow cytometry. *Curr Protoc Immunol* 2017;119(01):5.7.1–5.7.20
- 4 Darzynkiewicz Z. Critical aspects in analysis of cellular DNA content. *Curr Protoc Cytom* 2011;56(01):7.2.1–7.2.8
- 5 Darzynkiewicz Z. Critical aspects in analysis of cellular DNA content. *Curr Protoc Cytom* 2010;52(01):7.2.1–7.2.8
- 6 Poot M. Nucleic acid probes. *Curr Protoc Cytom* 2003;26(01):4.3.1–4.3.10
- 7 Vindeløv LL, Christensen IJ. A review of techniques and results obtained in one laboratory by an integrated system of methods designed for routine clinical flow cytometric DNA analysis. *Cytometry* 1990;11(07):753–770
- 8 Gupta N, Parihar M, Banerjee S, et al. FxCycle™ based ploidy correlates with cytogenetic ploidy in B-cell acute lymphoblastic leukemia and is able to detect the aneuploid minimal residual disease clone. *Cytometry B Clin Cytom* 2019;96(05):359–367
- 9 Bommannan K, Arumugam JR, Koshy T, Radhakrishnan V, Sagar TG, Sundersingh S. Blast size-specific flowcytometric ploidy assessment using FxCycle™ Violet dye and its correlation with conventional cytogenetic ploidy in pediatric precursor B-lineage acute lymphoblastic leukemia patients. *Int J Lab Hematol* 2021;43(04):760–770
- 10 Tembhare P, Badrinath Y, Ghogale S, et al. A novel and easy FxCycle™ violet based flow cytometric method for simultaneous assessment of DNA ploidy and six-color immunophenotyping. *Cytometry A* 2016;89(03):281–291
- 11 Smets LA, Slater R, van Wering ER, et al. DNA index and %S-phase cells determined in acute lymphoblastic leukemia of children: a report from studies ALL V, ALL VI, and ALL VII (1979–1991) of the Dutch Childhood Leukemia Study Group and The Netherlands Workgroup on Cancer Genetics and Cytogenetics. *Med Pediatr Oncol* 1995;25(06):437–444
- 12 Tsurusawa M, Katano N, Fujimoto T, eds. Prognosis and DNA aneuploidy in children with acute lymphoblastic leukemia. In: *Acute Leukemias II: Prognostic Factors and Treatment Strategies*. Berlin: Springer; 1990:174–181
- 13 Rachieru-Sourisseau P, Baranger L, Dastugue N, et al. DNA Index in childhood acute lymphoblastic leukaemia: a karyotypic method to validate the flow cytometric measurement. *Int J Lab Hematol* 2010;32(03):288–298
- 14 Mrózek K, Harper DP, Aplan PD. Cytogenetics and molecular genetics of acute lymphoblastic leukemia. *Hematol Oncol Clin North Am* 2009;23(05):991–1010, v
- 15 Swerdlow S, Campo E, Harris NL, et al. WHO Classification of Tumours of Haematopoietic and Lymphoid Tissues. Rev. 4th ed. IARC: Lyon; 2017:421
- 16 Haas OA, Borkhardt A. Hyperdiploidy: the longest known, most prevalent, and most enigmatic form of acute lymphoblastic leukemia in children. *Leukemia* 2022;36(12):2769–2783
- 17 Look AT, Roberson PK, Williams DL, et al. Prognostic importance of blast cell DNA content in childhood acute lymphoblastic leukemia. *Blood* 1985;65(05):1079–1086
- 18 Duque RE, Andreeff M, Braylan RC, Diamond LW, Peiper SC. Consensus review of the clinical utility of DNA flow cytometry

- in neoplastic hematopathology. *Cytometry* 1993;14(05):492–496
- 19 Cervantes E, Enriquez DJ, Vidal J, Retamozo R. Prognostic value of DNA index by flow cytometry for minimal residual disease in childhood b-cell acute lymphoblastic leukemia. *Blood* 2018;132:5287
  - 20 Forestier E, Holmgren G, Roos G. Flow cytometric DNA index and karyotype in childhood lymphoblastic leukemia. *Anal Cell Pathol* 1998;17(03):145–156
  - 21 Yu C-H, Lin T-K, Jou S-T, et al. MLPA and DNA index improve the molecular diagnosis of childhood B-cell acute lymphoblastic leukemia. *Sci Rep* 2020;10(01):11501
  - 22 Pérez-Vera P, Frías S, Carnevale A, et al. A strategy to detect chromosomal abnormalities in children with acute lymphoblastic leukemia. *J Pediatr Hematol Oncol* 2004;26(05):294–300
  - 23 Dastugue N, Suciú S, Plat G, et al. Hyperdiploidy with 58–66 chromosomes in childhood B-acute lymphoblastic leukemia is highly curable: 58951 CLG-EORTC results. *Blood* 2013;121(13):2415–2423
  - 24 Safavi S, Paulsson K. Near-haploid and low-hypodiploid acute lymphoblastic leukemia: two distinct subtypes with consistently poor prognosis. *Blood* 2017;129(04):420–423
  - 25 Pui C-H, Reborá P, Schrappe M, et al; Ponte di Legno Childhood ALL Working Group. Outcome of children with hypodiploid acute lymphoblastic leukemia: a retrospective multinational study. *J Clin Oncol* 2019;37(10):770–779
  - 26 Charrin C, Thomas X, Ffrench M, et al. A report from the LALA-94 and LALA-SA groups on hypodiploidy with 30 to 39 chromosomes and near-triploidy: 2 possible expressions of a sole entity conferring poor prognosis in adult acute lymphoblastic leukemia (ALL). *Blood* 2004;104(08):2444–2451
  - 27 Ma SK, Chan GC, Wan TS, et al. Near-haploid common acute lymphoblastic leukaemia of childhood with a second hyperdiploid line: a DNA ploidy and fluorescence in-situ hybridization study. *Br J Haematol* 1998;103(03):750–755
  - 28 Barilà G, Bonaldi L, Grassi A, et al. Identification of the true hyperdiploid multiple myeloma subset by combining conventional karyotyping and FISH analysis. *Blood Cancer J* 2020;10(02):18
  - 29 Lima M, Teixeira MdosA, Fonseca S, et al. Immunophenotypic aberrations, DNA content, and cell cycle analysis of plasma cells in patients with myeloma and monoclonal gammopathies. *Blood Cells Mol Dis* 2000;26(06):634–645
  - 30 San Miguel JF, García-Sanz R, González M, et al. A new staging system for multiple myeloma based on the number of S-phase plasma cells. *Blood* 1995;85(02):448–455
  - 31 Zhan F, Huang Y, Colla S, et al. The molecular classification of multiple myeloma. *Blood* 2006;108(06):2020–2028
  - 32 Rajan AM, Rajkumar SV. Interpretation of cytogenetic results in multiple myeloma for clinical practice. *Blood Cancer J* 2015;5(10):e365–e
  - 33 Debes-Marun CS, Dewald GW, Bryant S, et al. Chromosome abnormalities clustering and its implications for pathogenesis and prognosis in myeloma. *Leukemia* 2003;17(02):427–436
  - 34 Fonseca R, Barlogie B, Bataille R, et al. Genetics and cytogenetics of multiple myeloma: a workshop report. *Cancer Res* 2004;64(04):1546–1558
  - 35 Sidana S, Jevremovic D, Ketterling RP, et al. Rapid assessment of hyperdiploidy in plasma cell disorders using a novel multiparametric flow cytometry method. *Am J Hematol* 2019;94(04):424–430
  - 36 Scarffe JH, Hann IM, Evans DI, et al. Relationship between the pretreatment proliferative activity of marrow blast cells and prognosis of acute lymphoblastic leukaemia of childhood. *Br J Cancer* 1980;41(05):764–771
  - 37 Pierzyna-Świtaiła M, Sędek Ł, Kulis J, et al. Multicolor flow cytometry immunophenotyping and characterization of aneuploidy in pediatric B-cell precursor acute lymphoblastic leukemia. *Cent Eur J Immunol* 2021;46(03):365–374
  - 38 Kumar BK, Bhatia P, Trehan A, Singh AP, Kaul D, Bansal D. DNA ploidy and S-phase fraction analysis in paediatric b-cell acute lymphoblastic leukemia cases: a tertiary care centre experience. *Asian Pac J Cancer Prev* 2015;16(17):7917–7922
  - 39 Trendle MC, Leong T, Kyle RA, et al. Prognostic significance of the S-phase fraction of light-chain-restricted cytoplasmic immunoglobulin (cIg) positive plasma cells in patients with newly diagnosed multiple myeloma enrolled on Eastern Cooperative Oncology Group treatment trial E9486. *Am J Hematol* 1999;61(04):232–237
  - 40 Greipp PR, Witzig TE, Gonchoroff NJ. Immunofluorescent plasma cell labeling indices (LI) using a monoclonal antibody (BU-1). *Am J Hematol* 1985;20(03):289–292
  - 41 Greipp P, Witzig T. Cell Kinetics in Plasma Cell Myeloma. *Manual of Clinical Laboratory Immunology*. 4th ed. Washington, DC: American Society of Microbiology; 1992:96–102
  - 42 Mikhael JR, Dingli D, Roy V, et al. Management of newly diagnosed symptomatic multiple myeloma: updated Mayo Stratification of Myeloma and Risk-Adapted Therapy (mSMART) consensus guidelines 2013. *Mayo Clin Proc* 2013;88(04):360–376
  - 43 Kumar SK, Mikhael JR, Buadi FK, et al. Management of newly diagnosed symptomatic multiple myeloma: updated Mayo Stratification of Myeloma and Risk-Adapted Therapy (mSMART) consensus guidelines. *Mayo Clin Proc* 2009;84(12):1095–1110
  - 44 Larsen JT, Chee CE, Lust JA, Greipp PR, Rajkumar SV. Reduction in plasma cell proliferation after initial therapy in newly diagnosed multiple myeloma measures treatment response and predicts improved survival. *Blood* 2011;118(10):2702–2707
  - 45 Orfão A, García-Sanz R, López-Berges MC, et al. A new method for the analysis of plasma cell DNA content in multiple myeloma samples using a CD38/propidium iodide double staining technique. *Cytometry* 1994;17(04):332–339
  - 46 Sidiqi MH, Aljama MA, Jevremovic D, et al. Plasma cell proliferative index predicts outcome in immunoglobulin light chain amyloidosis treated with stem cell transplantation. *Haematologica* 2018;103(07):1229–1234
  - 47 Aljama MA, Sidiqi MH, Lakshman A, et al. Plasma cell proliferative index is an independent predictor of progression in smoldering multiple myeloma. *Blood Adv* 2018;2(22):3149–3154
  - 48 Paiva B, Vídriales M-B, Montalbán M-Á, et al. Multiparameter flow cytometry evaluation of plasma cell DNA content and proliferation in 595 transplant-eligible patients with myeloma included in the Spanish GEM2000 and GEM2005<65y trials. *Am J Pathol* 2012;181(05):1870–1878
  - 49 Shankey TV, Rabinovich P, Bagwell B, et al. Guidelines for implementation of clinical DNA cytometry. *International Society for Analytical Cytology. Cytometry* 1993;14(05):472–477
  - 50 Pozarowski P, Darzynkiewicz Z. Analysis of cell cycle by flow cytometry. *Methods Mol Biol* 2004;281:301–311
  - 51 Darzynkiewicz Z, Juan G, Srouf EF. Differential staining of DNA and RNA. *Curr Protoc Cytom* 2004;7(01):7.3.1–7.3.16
  - 52 Tembhare P, Badrinath Y, Ghogale S, Subramanian PG. Method for DNA Ploidy analysis along with Immunophenotyping for rare populations in a sample using FxCycle violet. *Curr Protoc Cytom* 2017;80(01):6.38.1–6.38.15
  - 53 Han-Shu F, Ming-Fei L, Jing S. New methods for cell cycle analysis. *Chin J Anal Chem* 2019;47(09):1293–1301
  - 54 Tomono A, Itoh T, Yanagita E, Imagawa N, Kakeji Y. Cell cycle kinetic analysis of colorectal neoplasms using a new automated immunohistochemistry-based cell cycle detection method. *Medicine (Baltimore)* 2015;94(04):e501
  - 55 Ismail IH, Hendzel MJ. The  $\gamma$ -H2A.X: is it just a surrogate marker of double-strand breaks or much more? *Environ Mol Mutagen* 2008;49(01):73–82



- 56 Nath J, Johnson KL. A review of fluorescence in situ hybridization (FISH): current status and future prospects. *Biotech Histochem* 2000;75(02):54–78
- 57 Sakaue-Sawano A, Kurokawa H, Morimura T, et al. Visualizing spatiotemporal dynamics of multicellular cell-cycle progression. *Cell* 2008;132(03):487–498
- 58 Dubrovsky JG, Ivanov VB. Celebrating 50 years of the cell cycle. *Nature* 2003;426(6968):759
- 59 Spitzer MH, Nolan GP. Mass cytometry: single cells, many features. *Cell* 2016;165(04):780–791
- 60 Yoo HJ, Park J, Yoon TH. High throughput cell cycle analysis using microfluidic image cytometry ( $\mu$ FIC). *Cytometry A* 2013;83(04):356–362
- 61 Tian X, Zhang Y. Research progress of Raman spectroscopy in the diagnosis of early lung cancer. *Zhongguo Fei Ai Za Zhi* 2018;21(07):560–564
- 62 de Beer MA, Giepmans BNG. Nanobody-based probes for subcellular protein identification and visualization. *Front Cell Neurosci* 2020;14:573278